Polymer 51 (2010) 4958–4968

Contents lists available at ScienceDirect

Polymer

journal homepage: www.elsevier.com/locate/polymer

A facile route for preparing stable co-continuous morphology of LLDPE/PA6 blends with low PA6 content

Hengchong Shi [a], Dean Shi [b,c,*], Xiaoyang Wang [b], Ligang Yin [a], Jinghua Yin [a,**], Yiu-Wing Mai [c,***]

[a] State Key Laboratory of Polymer Physics and Chemistry, Changchun Institute of Applied Chemistry, Chinese Academy of Sciences, Changchun 130022, PR China
[b] Ministry-of-Education Key Laboratory for the Green Preparation and Application of Functional Materials, Faculty of Materials Science and Engineering, Hubei University, Wuhan 430062, PR China
[c] Centre for Advanced Materials Technology (CAMT), School of Aerospace, Mechanical and Mechatronic Engineering J07, The University of Sydney, Sydney, NSW 2006, Australia

ARTICLE INFO

Article history:
Received 15 June 2010
Received in revised form
29 July 2010
Accepted 12 August 2010
Available online 19 August 2010

Keywords:
LLDPE
PA6
Co-continuous morphology

ABSTRACT

A facile method is employed to prepare a series of LLDPE/PA6 blends with co-continuous morphology with low PA6 content via reactive extrusion. In these blends, co-continuous morphology is obtained by introducing graft copolymers with both high and low molecular weight trunk chains to the interface simultaneously. Maleic anhydride functionalized polybutadine (PB-g-MAH, $\overline{M}_n \approx 3000$g/mol and MAH content = 10 wt%) is first melt grafted onto the LLDPE backbones with dicumyl peroxide (DCP) as an initiator. Part of PB-g-MAH is grafted onto LLDPE to form LLDPE-g-PB-g-MAH copolymer. During reactive extrusion, *in-situ* formed Copolymer II (polybutadiene-graft-polyamide, PB-g-PA6) with a low molecular weight trunk chain (PB) is obtained from the reaction between the maleic anhydride group of free or non-grafted PB-g-MAH and the amino group on PA6 molecules; while Copolymer I (LLDPE-g-PB-g-PA6) is obtained via the reaction between the maleic anhydride group of the grafted PB-g-MAH (i.e., LLDPE-g-PB-g-MAH) and the amino group of PA6. Copolymer I with a high molecular weight trunk chain, LLDPE, should strengthen the interface and favor stress transfer, enabling the deformation of PA6; and Copolymer II (PB-g-PA6) with a low molecular weight trunk chain, PB, facilitates the formation of a flat interface between LLDPE and PA6, thus promoting an elongated PA6 phase. Therefore, co-continuous morphology of LLDPE/PA6 blend is successfully prepared with only 25 wt% PA6 by controlling suitable amounts of Copolymers I and II in the blend.

1. Introduction

Polymer blends have become an important route to new, high-performance polymeric materials over the past 40 years. The technique of blending polymers can serve many different purposes. Recently, there is an increasing interest in blends with co-continuous morphology. Compared to the blends with a droplet-in-matrix morphology, blends with a co-continuous morphology can possess better combinations of properties from the components [1,2]. For example, a co-continuous structure confers maximum contribution to the elastic modulus from each component [2–4] and yields a synergistic effect on the impact properties [5–7]. Polymer blends with a co-continuous morphology are also used to prepare porous materials [8–11], which have wide potential applications in water filtration and controlled drug release.

One way to achieve co-continuous structures is by synthesis of interpenetrating molecular networks [12,13]. This level of mixing can only be achieved by simultaneous or sequential chemical synthesis of the polymers themselves and can only be realized in certain limited polymer pairs. For miscible polymer systems, co-continuous structures can be formed during the demixing process by spinodal decomposition [3]. This so-called thermal induced phase separation (TIPS) method is still widely used in preparing porous polymer films [14–16] and hollow polymer fibers [17,18]. However, most industrially useful polymer pairs with high molecular weights are completely immiscible systems without a miscible region under melt mixing conditions. Since the 1970's, it was believed that, for immiscible polymer blends, co-continuous

* Corresponding author. Ministry-of-Education Key Laboratory for the Green Preparation and Application of Functional Materials, Faculty of Materials Science and Engineering, Hubei University, Wuhan 430062, PR China.
** Corresponding author. State Key Laboratory of Polymer Physics and Chemistry, Changchun Institute of Applied Chemistry, Chinese Academy of Sciences, Changchun 130022, PR China.
*** Corresponding author. Centre for Advanced Materials Technology (CAMT), School of Aerospace, Mechanical and Mechatronic Engineering J07, The University of Sydney, Sydney, NSW 2006, Australia.
E-mail addresses: deanshi2001@yahoo.com (D. Shi), yinjh@ciac.jl.cn (J. Yin), yiu-wing.mai@sydney.edu.au (Y.-W. Mai).

0032-3861/$ – see front matter © 2010 Elsevier Ltd. All rights reserved.
doi:10.1016/j.polymer.2010.08.023

morphologies are mainly formed close to the phase inversion point [19–21]. Later studies revealed a narrow composition range in which co-continuous morphologies can be formed in binary immiscible polymer blends [22–24]. Based on the sheet-forming mechanism of melt blending proposed by Macosko et al. [25,26], elongated sheet or droplets of the dispersed phase should be formed during the melt mixing process. Willemse et al. suggested that the key point for a co-continuous morphology is the stability and coalescence ability of such elongated particles [27,28]. The lower is the interfacial tension, the more stable are the elongated droplets [29]. Therefore, it is only practical to obtain co-continuous polymer blends from polymer pairs with relatively low interfacial tension, such as PP/PE/EPR blends [30], PS/PMMA blends [31], PC/PMMA [32] and PP/EPDM [33], etc. In polymer blends with immiscible polymer pairs which have high interfacial tension, premade [34,35] or *in-situ* formed copolymers [36–39] are often used as compatibilizers to reduce the interfacial tension and enhance the compatibility. However, since the existence of compatibilizers reduces not only the interfacial tension but also the probability of coalescence between dispersed particles [27,28,40,41], the formation of a co-continuous morphology which requires low interfacial tension and high coalescence probability of the dispersed particles will similarly be prohibited. Hence, even though the addition of the compatibilizers can stabilize the formed morphologies, it will further narrow down the composition range to form a co-continuous micro-emulsion in the immiscible polymer blends with high interfacial tension [42,43].

Recently, Pernot et al. [4] demonstrated a new method using the copolymer as a "skeleton" rather than a compatibilizer in the co-continuous system in their pioneering study. In that work, the copolymer molecules should have a symmetric structure and could form a co-continuous morphology [44–46] which behaved like a "sponge" and could dissolve the low molecular weight un-reacted chains to form interfaces with large radii of curvature. Hence, the molecular weight of the copolymer should be higher than each homopolymer. In their co-continuous PE-MAH/PA6 blends, only PA6 with very low molecular weight was used (2500 g/mol for PA6). Following this method, Pu et al. [47] successfully prepared co-continuous PS/PMMA blends with only 30 wt% PS by adding random copolymer PS-b-P(S-ran-MMA) in the system. Although these strict protocols are hardly satisfied in the commercial polymer systems, Pernot et al.'s study provided a hint of new methods to prepare co-continuous immiscible polymer blends with low minor phase content – forming an interface as flat as can be. Based on previous investigations on copolymer self-assembly [48–50], the comb-like or Y-shaped copolymer with a trunk chain A and a graft chain B, which is often *in-situ* formed in reactive compatibilization of polymer blends, is favored to adopt a flat interface only if $0.85 \geq \varphi_B \geq 0.67$ at $\epsilon \approx 2$, where ϕ_B is volume fraction of graft B and $\epsilon = (n_A/n_B)/(I_A/I_B)^{1/2}$ (n_A and n_B are arm numbers of A and B blocks which represent the asymmetry owing to the molecular architecture, and $I_i (i = A \text{ or } B)$is the ratio of the segment volume to the square of statistical segment length for the ith block. The factor $(I_A/I_B)^{1/2}$ shows the conformational asymmetry between the two block materials). In commercial immiscible polymer pairs, most *in-situ* formed copolymers via the reactive compatibilization process are Y-shaped ($\epsilon \approx 2$) because of the existing large molecular weight and low reactive group contents. In this case, the molecular weight of polymer B should be much larger than that of polymer A so that the *in-situ* formed Y-shaped copolymer with B graft will form a flat interface. However, this cannot be satisfied in most of the immiscible polymer pairs. Sphere-like morphology is most common in most Y-shaped copolymers [51,52]. Another difficulty is that though copolymers with low molecular weight trunk chains have smaller steric hindrance to the coalescence between the dispersed particles, which is conducive to the formation of a co-continuous morphology [53], it will also reduce very much the interfacial strength and inhibit the stress transfer between different phases. The dispersion of the minor phase in the matrix should be difficult and result in large dispersion phase size. Both theoretical [54,55] and experimental [56,57] studies showed that copolymers with large molecular weight should have better efficiency in compatibilization than those with low molecular weight. Thus, only the presence of *in-situ* formed copolymers with low molecular weight trunk chains is still insufficient to form a co-continuous morphology in the immiscible polymer blends. In addition, copolymers with low molecular weight trunk chains located at the interface will also reduce the stability of this morphology during further processing. A co-continuous morphology can be coarsened and even changed to a droplet-in-matrix morphology after annealing at high temperatures [21,58]. Therefore, a compromised way to prepare blends with a co-continuous morphology at low minor phase content might be successful if a suitable amount of graft copolymers with both high and low molecular weight trunk chains can exist simultaneously in the system. In this work, we report a facile method to prepare co-continuous LLDPE/PA6 blends with low PA6 content via reactive extrusion by controlling the contents and structures of *in-situ* formed graft copolymers with different molecular weights. This co-continuous morphology is stable enough and can be preserved when subjected to further processing.

2. Experimental

2.1. Materials

Linear low density polyethylene (LLDPE, $\overline{M}_n \approx 20000$g/mol) was supplied by Daqing Petroleum & Chemical Co. Low molecular weight functionalized rubber, polybutadiene grafted with maleic anhydride (PB-g-MAH, $\overline{M}_n \approx 3000$g/mol, MAH is 10 wt%) was provided by Yanshan Petroleum & Chemical Co. Nylon 6 (PA6-M2800, $\overline{M}_n \approx 20000$g/mol) and LLDPE-g-MAH (MAH is 1.0 wt%) were bought from Guangdong Xinhuimeida Co. and Beijing Sunred Plastics Co., respectively. Dicumyl peroxide (DCP) was purchased from Beijing Chemical Agent Co. All materials were used as-received.

2.2. Blend preparation

2.2.1. Method I

Low molecular weight PB-g-MAH was first melt blended with LLDPE by a HAAKE PolyLab co-rotating twin-screw extruder at 190 °C with DCP as initiator. Part of PB-g-MAH was grafted to the LLDPE backbones and formed LLDPE-g-PB-g-MAH. The concentration of MAH in each sample was determined by chemical titration [59]. The grafting degree of PB-g-MAH on LLDPE backbones in different samples was calculated based on the MAH concentration in PB-g-MAH (10 wt%). The results were listed in Table 1. The mixture of pre-modified LLDPE (LLDPE/LLDPE-g-PB-g-MAH/PB-g-MAH) was further blended with PA6 in the HAAKE co-rotating twin-screw extruder or an internal batch mixer at 230 °C (PA6 is

Table 1
Pre-modified LLDPE samples.

Sample	Total PB-g-MAH content (wt%)	Grafted PB-g-MAH content (wt%)
LLDPEg10	10	4.8
LLDPEg5	5	2.5
LLDPEg3	3	1.3

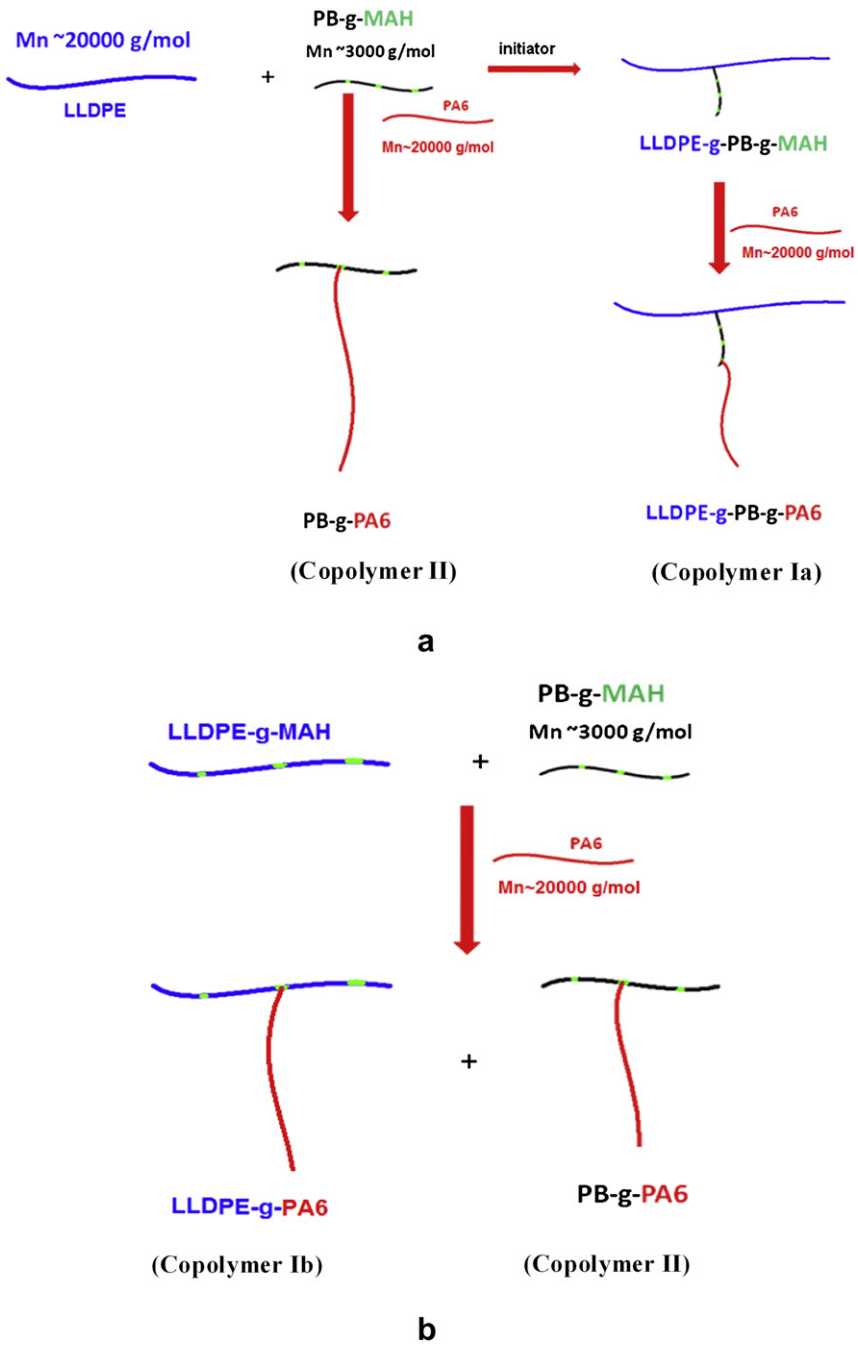

Scheme 1. Formation mechanisms of Copolymer I and Copolymer II by (a) Method I; and (b) Method II.

minor phase). During melt blending, the MAH groups in the pre-modified LLDPE reacted with the end amino groups in PA6 to form Y-shaped graft copolymers (see Scheme 1a). Here, there are two kinds of Y-shaped graft copolymers formed, both of which have PA6 grafts. One (Copolymer Ia) has PE as the trunk chain and the other (Copolymer II) has PB as the trunk chain. In our materials system, since the molecular weights and densities of PB and PA6 are: $\overline{M}_{nPB} \approx 3000$g/mol, $M_n \approx 20000$g/mol and ρ_{PB}=0.9 g/cm^3, ρ_{PA6}=1.14 g/cm^3, respectively, the theoretical volume fraction of PA6 in Copolymer II is calculated as $\varphi_{PA6} \approx 0.84$. Taking the degradation of PA6 and crosslink of PB during the melt blending process, the actual volume fraction of PA6 grafts in Copolymer II should be slightly lower than 0.84. This puts it right within the theoretical range 0.67–0.85 to form lamellar morphology [48,50,53]. Therefore, it can be concluded that the existence of Copolymer II at the interface should facilitate the formation of a flat interface with large radius or low curvature, which favors the co-continuous morphology without the minor phase content reaching the phase inversion point. The existence of a certain amount of Copolymer Ia with long trunk chains in the system will induce fine dispersion of PA6 and largely alleviate the disadvantages of Copolymer II for formation of a stable co-continuous morphology. The formation and stability of the co-continuous LLDPE/PA6 blends with low PA6 content should be tailored by meticulously controlling the content and content ratio of Copolymers Ia and II in this system. Unlike blends obtained by the internal batch mixer, the pellets obtained by the HAAKE co-

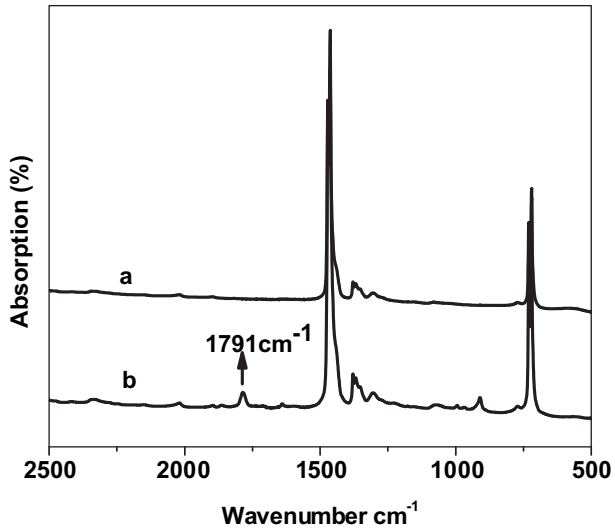

Fig. 1. FTIR spectra of (a) LLDPE and (b) LLDPEg10 (non-grafted PB-g-MAH is removed).

rotating twin-screw extruder were further cast into thin films ~0.5 mm thick using a HAAKE single screw extruder and a three-roller accessory before characterization.

2.2.2. Method II

LLDPE-g-MAH was used to replace the LLDPE-g-PB-g-MAH in Method I. So, certain amounts of LLDPE-g-MAH, PB-g-MAH and PA6 were mixed directly in the internal mixer at 230 °C (PA6 is the minor phase). Copolymer Ib was formed by the reaction between MAH on LLDPE-g-MAH and the end amino group in PA6, while Copolymer II came from the reaction of MAH on the PB-g-MAH molecules. The content ratios of Copolymers Ib and II were changed by varying the content of LLDPE-g-MAH and PB-g-MAH. The mechanism was shown in Scheme 1b.

For simplicity, hereafter, only Copolymer I, instead of Copolymer Ia and Ib, was used to represent the *in-situ* formed copolymer with a large molecular weight trunk chain.

2.3. Solvent extraction

LLDPE and PA6 in the samples were extracted via their selective solvent xylene and formic acid, respectively. For extraction of LLDPE, the sample was immerged in xylene at 110 °C; and for PA6, this occurred in formic acid solution at 60 °C. All the samples were extracted to constant weight. The sample weight loss was calculated by:

$$\%\text{weight loss} = \frac{W_{\text{initial}} - W_{\text{final}}}{W_{\text{initial}}} \times 100\%$$

2.4. Rheological measurement

Rheological properties of polymer blends were measured with an MCR-300 (Physica) Rheometer using 25 mm diameter parallel plates. Frequency sweeps of 0.1–100 rad/s were performed at 235 °C and a strain of 5% in nitrogen.

2.5. Thermal and dynamic mechanical analysis

The crystallization of PA6 in different blends was studied by using differential scanning calorimetry (DSC) measurements on

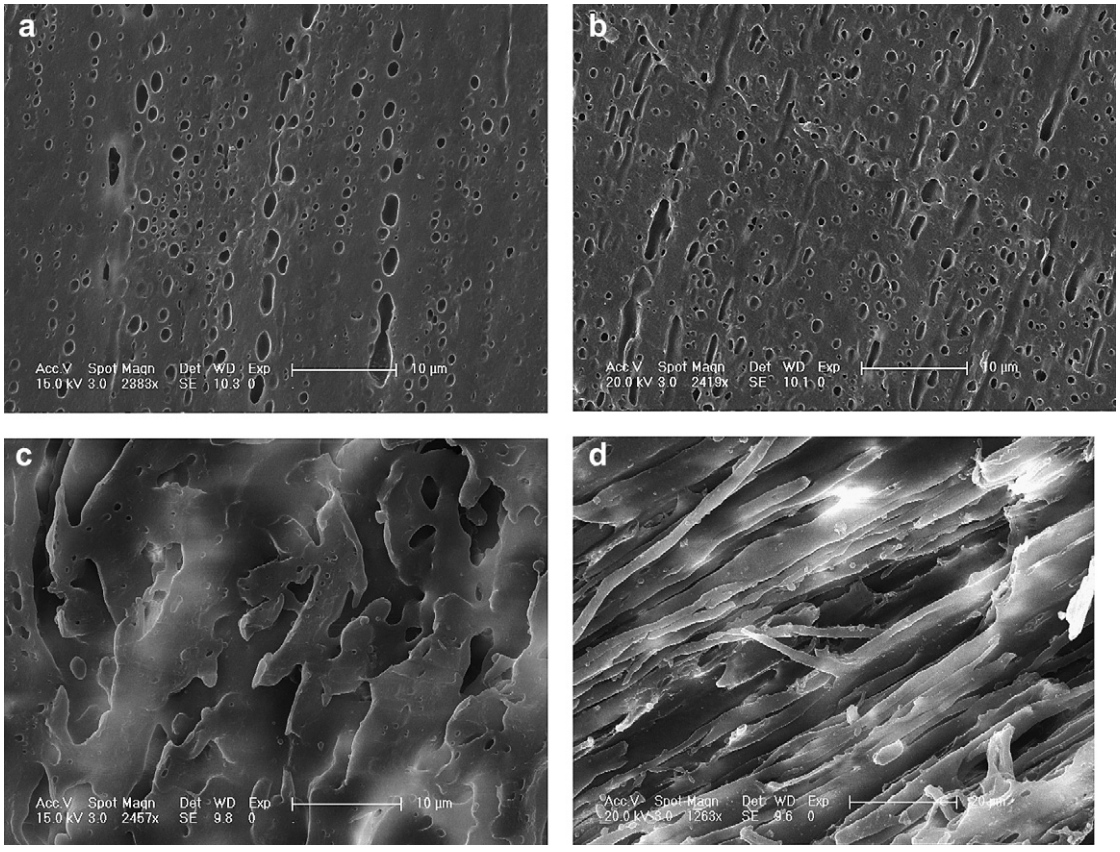

Fig. 2. SEM micrographs of LLDPEg10/PA6 films (extracted by formic acid)-parallel to flow direction: (a) PA6 10 wt%; (b) PA6 20 wt%; (c) PA6 25 wt%; and (d) PA6 30 wt%.

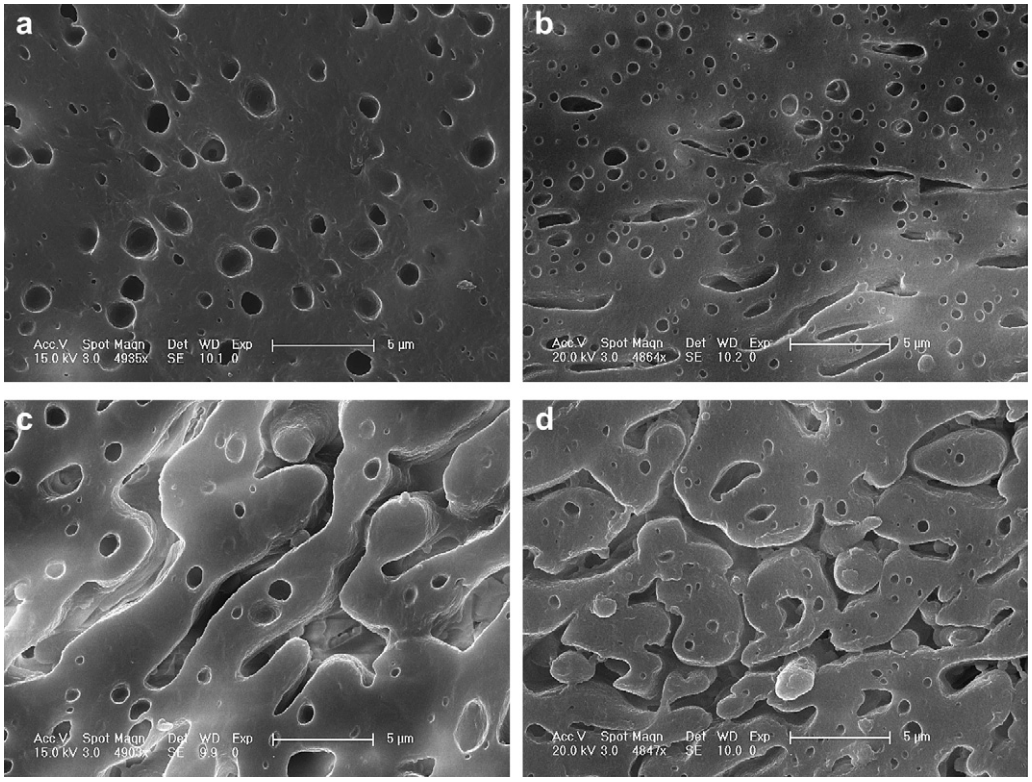

Fig. 3. SEM micrographs of LLDPEg10/PA6 films (extracted by formic acid) – transverse to flow direction: (a) PA6 10 wt%; (b) PA6 20 wt%; (c) PA6 25 wt%; and (d) PA6 30 wt%.

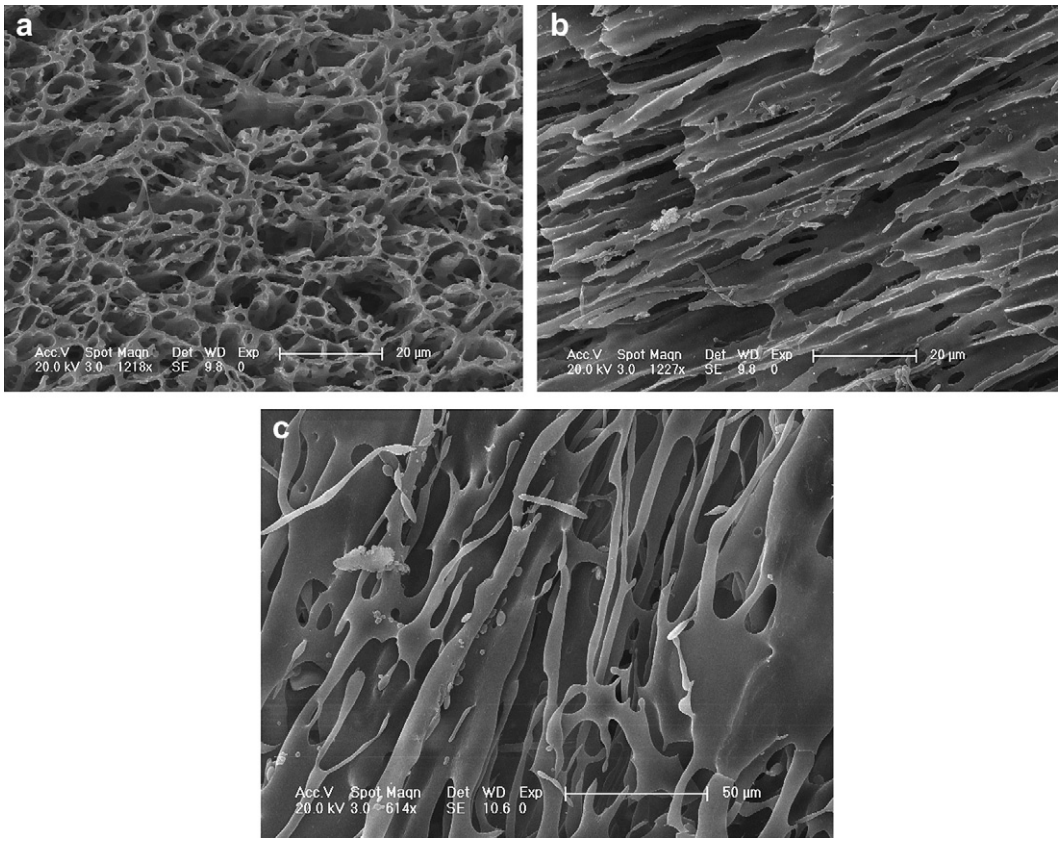

Fig. 4. SEM micrographs of LLDPEg10/PA6 (70/30 wt/wt) film (extracted by xylene): (a) transverse to flow direction; (b) parallel to flow direction; and (c) parallel to flow direction (with further annealing in heat compression mold at 235 °C for 0.25 h).

a TA Instrument DSC Q100 apparatus. Samples were heated to 250 °C and held for 3 min to erase any thermal history, and then cooled to 25 °C at a rate of 10 °C/min. Tensile mode DMA tests of the blends were performed with a DMA2980 (TA instruments) (amplitude 3 μm and frequency 10 Hz). The rectangular samples measured 10 × 5 × 0.3 mm^3. Data were recorded from −100 to 200 °C at a rate of 3 °C/min under nitrogen flow. The storage (or elastic) modulus (E′) and loss tangent (tan δ) were obtained as functions of temperature.

2.6. Morphology analysis

TEM micrographs were taken on a TEM-Zeiss EM 900 transmission electron microscope (Zeiss, Germany) operating at an accelerating voltage of 80 kV. Ultra-thin specimens were cut by ultra-microtomy with a diamond knife at −120 °C. An aqueous solution of phosphotungstic acid (PTA) was used to selectively stain the PA6 phase in the blend, which would show a darker image. SEM micrographs were also obtained with a field emission scanning electron microscope (FESEM; XL 30, FEI Company) at a voltage between 15 and 20 kV. The sample surfaces were first microtomed under liquid nitrogen with a Leica microtome equipped with a glass knife. Then, the microtomed samples were treated to a solvent extraction step before coated with gold.

3. Results and discussion

In Method I, three pre-modified LLDPE with different content of PB-g-MAH are listed in Table 1. The new absorption peak at 1791 cm^{-1} in the purified grafted sample shown in the FTIR spectra (Fig. 1b) indicates that part of PB-g-MAH was actually grafted onto the LLDPE backbones. In all these pre-modified LLDPE samples, the content ratios between grafted and non-grafted PB-g-MAH were almost equal to 1:1. Although the content of *in-situ* formed graft copolymers with PA6 grafts could not be directly detected in this system, assuming the content ratios between Copolymer I and II are constant in the blends with these three pre-modified LLDPE is reasonable. In this case, only the effects of the total amount rather than the content ratio of Copolymer I and II on the blends morphology are studied.

Figs. 2 and 3 show SEM micrographs of LLDPEg10/PA6 films prepared by the Haake extruder with different PA6 contents. The morphologies along (Fig. 2) and perpendicular (Fig. 3) to the flow directions were recorded. When PA6 content was only 10 wt% (Figs. 2a and 3a), a full droplet-in-matrix morphology was observed. When the PA6 content was increased to 20 wt% (Figs. 2b and 3b) some elongated morphologies could be found. Fully co-continuous morphologies were obtained when the PA6 contents were more than 25 wt% (Figs. 2(c,d) and 3(c,d)).

To ascertain whether the co-continuous morphologies shown in Figs. (2c,d) and (3c,d) were just two-dimension cylindrical morphologies or truly three-dimension co-continuous morphology, these samples were also extracted by xylene (selective solvent of LLDPE) at 120 °C. The sample with 10 wt% PA6 was completely disintegrated and that with 20 wt% PA6 was distorted. For samples with 25 and 30 wt% PA6, both their forms and sizes did not change much before and after the extraction. Fig. 4 shows the morphologies of the sample with 30 wt% PA6. It was found that the fibril PA6 phase was actually three-dimension co-continuous. Despite the fibril diameter of PA6 was increased to some extent after annealing the sample at 235 °C for 0.25 h (see Fig. 4c), the co-continuous morphology remained intact.

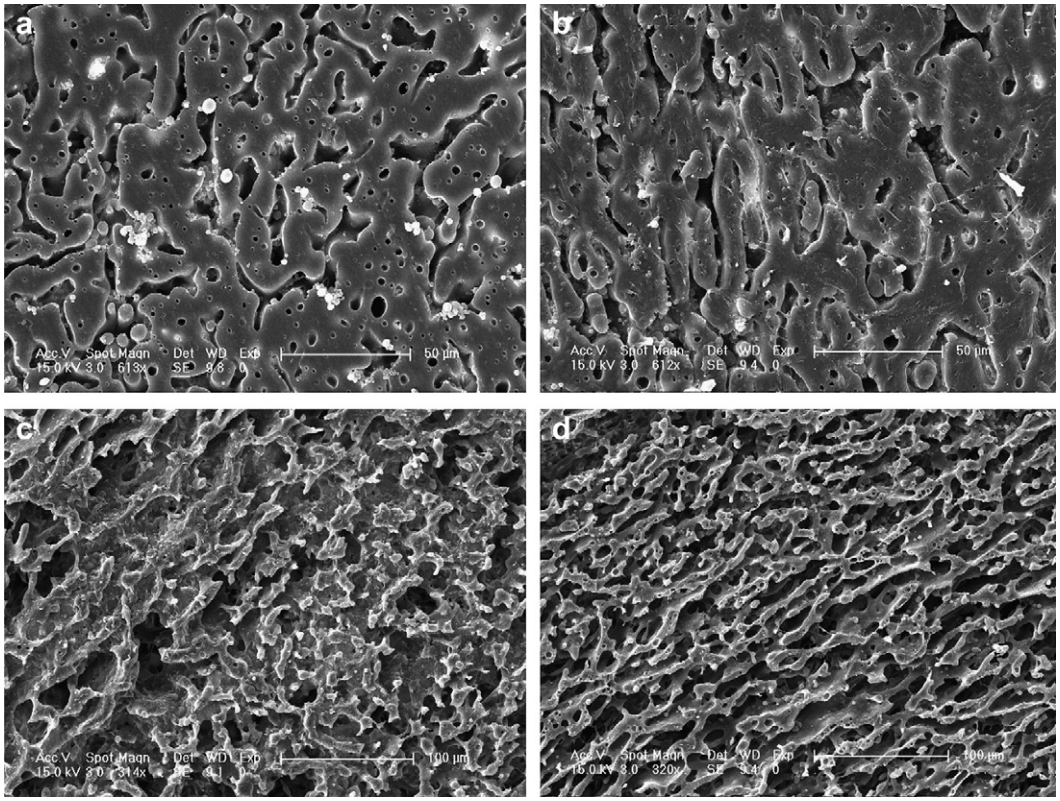

Fig. 5. SEM micrographs of LLDPEg10/PA6 (70/30 wt/wt) prepared by the internal batch mixer: (a) and (b) are extracted by formic acid; (c) and (d) are extracted by xylene. (a) and (c) are obtained with sample immediately immerged into liquid nitrogen to freeze the morphology after melt mixing; (b) and (d) are obtained with sample cooling at room temperature after melt mixing.

Did the film casting process enable the formation of co-continuous morphologies shown in Figs. 2 and 3? To answer this question, LLDPEg10/PA6 (70/30 wt/wt) blends were also prepared via the internal batch mixer with a screw speed of 50 rpm. The morphologies of the blends were shown in Fig. 5. Two kinds of samples were prepared to evaluate the stability of *in-situ* formed morphologies. One was obtained by immersing the sample immediately into liquid nitrogen to freeze the morphology after melt mixing and the other was cooling at room temperature after melt mixing.

Co-continuous morphology could be found in both the formic acid extracted and xylene extracted samples. There was no noticeable difference between the fast frozen and slow cooled down samples, which indicated the stability of the morphology. When comparing the phase size shown in Figs. 2 and 3, it is noted that the blend prepared by the internal batch mixer has a relatively larger phase size. This result proves that the processing condition has influenced the final morphology. However, in the LLDPE/PA6 blends, both processing methods (using co-rotating twin-screw extruder or internal batch mixer) yield the same co-continuous morphology.

Fig. 6 shows the morphologies of blends with the same PA6 content (30 wt%) but different amount of low molecular weight PB-g-MAH. When the total content of PB-g-MAH is 5 wt% and the free content of PB-g-MAH is 2.5 wt%, co-continuous morphology can still be seen in Fig. 6a. While in Fig. 6b, when the total content of PB-g-MAH is 3 wt% and free content of PB-g-MAH is only 1.7 wt%, the droplet-in-matrix morphology is formed. It is noted that when there is no free PB-g-MAH (Fig. 6c, LLDPE-g-MAH/PA6 blend) or the free PB-g-MAH in LLDPEg10 has been removed (Fig. 6d), the droplet-in-matrix morphology can be found. Similarly, if there is only free PB-g-MAH but no grafted PB-g-MAH, that is, only Copolymer II but no Copolymer I in the blends, the co-continuous morphology cannot happen (Fig. 6e). These results indicate that the co-existence of certain contents of both Copolymers I and II in the blends is the critical factor for the formation of the co-continuous morphology.

To further prove the above observations, LLDPE-g-MAH was used to replace directly the grafted LLDPE-g-PB-g-MAH to form Copolymer I in the LLDPE/PA6 blends (Method II). Copolymer II was also obtained from a certain amount of the low molecular weight

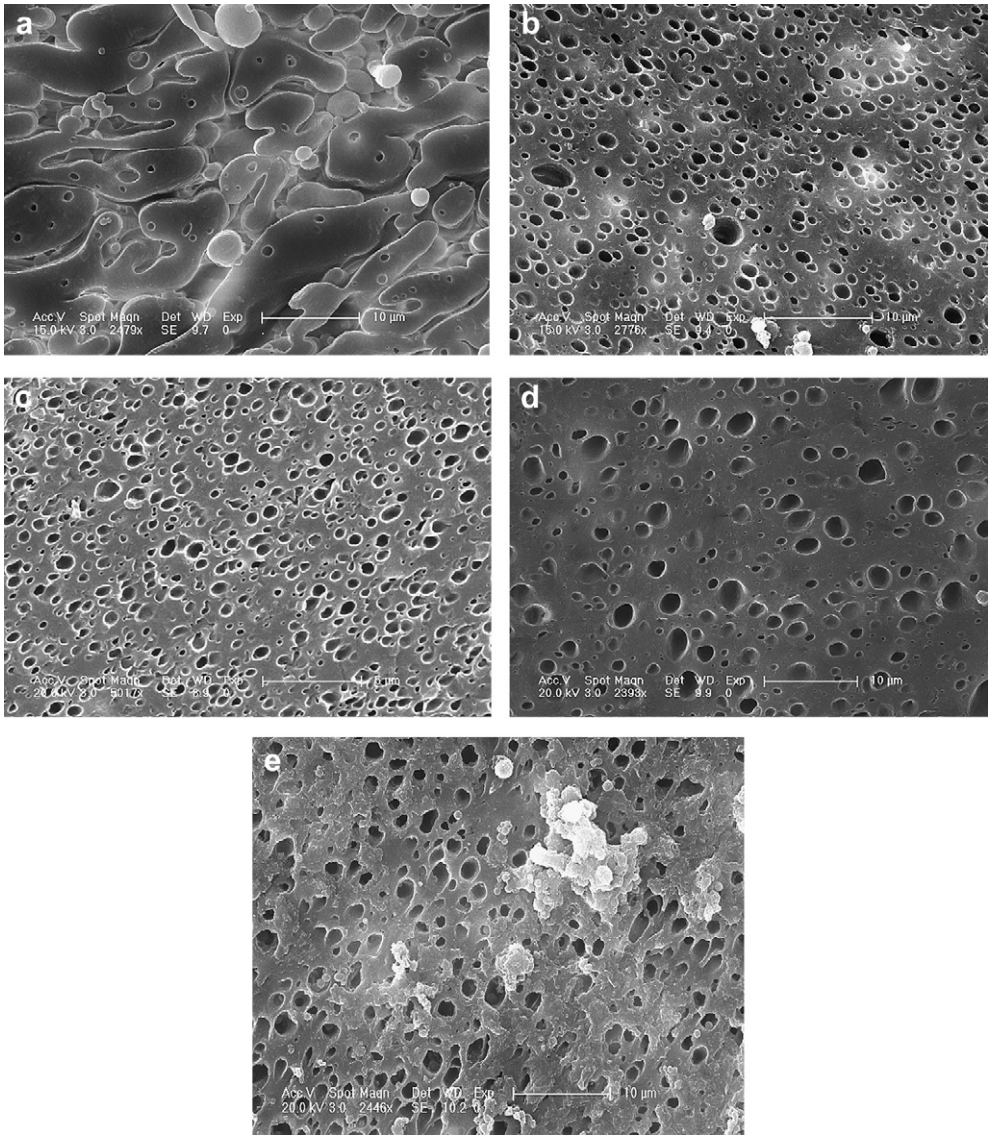

Fig. 6. SEM micrographs of different blends with 30 wt% of PA6: (a) LLDPEg5/PA6; (b) LLDPEg3/PA6; (c) PE-g-MAH/PA6; (d) LLDPEg10/PA6, non-grafted PB-g-MAH removed; and (e) (LLDPE/PB-g-MAH 95/5)/PA6 (extracted by formic acid).

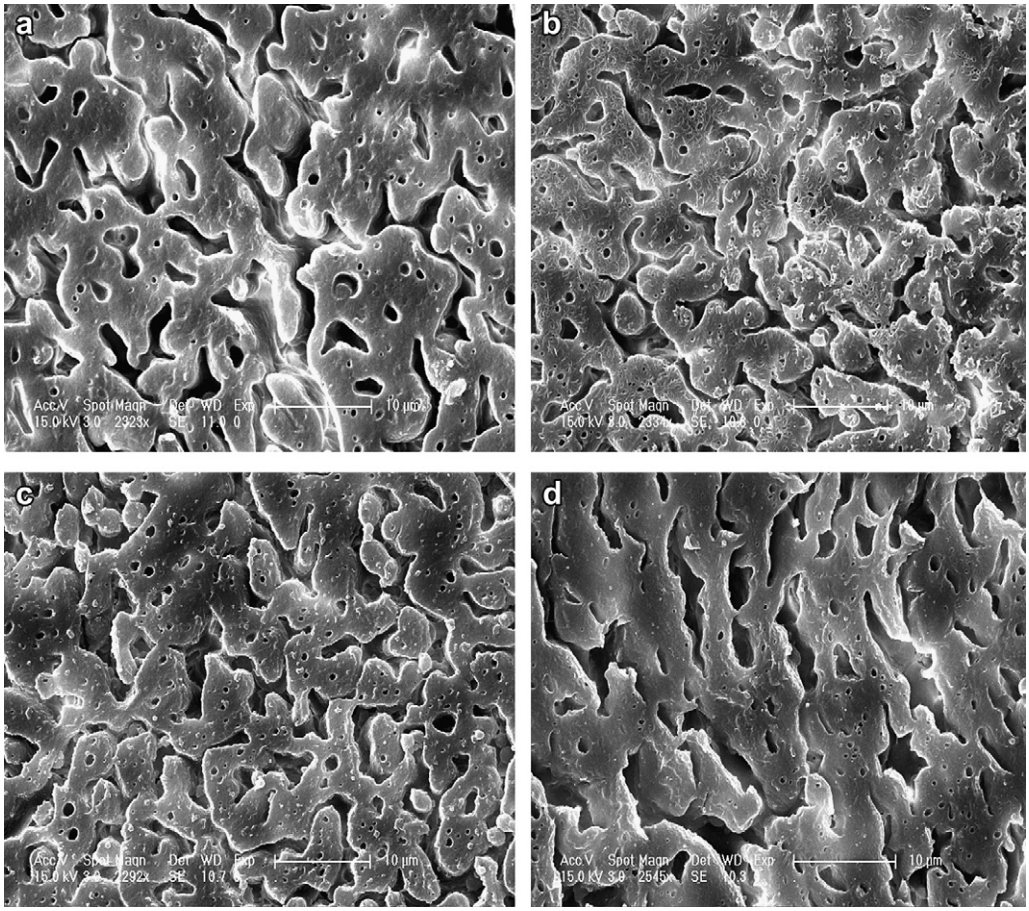

Fig. 7. SEM micrographs of different blends of LLDPE-g-MAH/PB-g-MAH/PA6 with 30 wt% PA6 (extracted by formic acid): (a) LLDPE-g-MAH/PB-g-MAH = 97/3; (b) LLDPE-g-MAH/PB-g-MAH = 95/5; (c) LLDPE-g-MAH/PB-g-MAH = 92/8; and (d) LLDPE-g-MAH/PB-g-MAH = 95/5 (annealed in compression mold at 235 °C for 0.25 h).

PB-g-MAH. All the samples were prepared by internal batch mixer at 235 °C. In these blends, PB-g-MAH was not grafted onto the LLDPE backbones. Their SEM micrographs (extracted by formic acid) are shown in Fig. 7. It can be seen that the co-continuous morphologies are formed in all the three blends with different PB-g-MAH contents (Fig. 7a–c). Furthermore, after the annealing process, even though the phase size increases to some extent, the co-continuous morphology remains unchanged (Fig. 7d).

It is acknowledged that only SEM micrographs are insufficient to confirm the formation of co-continuous morphology in polymer blends. A common and widely used method is solvent extraction method. If one phase is continuous in a polymer blend, it should be fully extracted by a selective solvent even it is the minor phase. Otherwise, only part of it can be extracted. If a selective solvent of the major phase is used, for blends with co-continuous morphologies, the residue continuous phase will stand still and the sample shape maintained. On the contrary, for blends with the droplet-in-matrix morphology, the sample will be disintegrated after the major continuous phase is removed. Hence, some samples studied were subjected to selective solvent extraction processes and the results are shown in Table 2. For all the blends with a co-continuous morphology (LLDPEg10/PA6:75/25, LLDPEg10/PA6:70/30, LLDPEg5/PA6:70/30), almost all the PA6 can be removed by formic acid. Also, these blends can retain their shape even after the major phase, LLDPE, is extracted. However, for those blends with a droplet-in-matrix morphology, only part of PA6 can be removed. The samples are disintegrated or distorted after LLDPE is removed. It is noted that for the samples with a co-continuous morphology, not all LLDPE is fully extracted, and the weights of extracted PA6 are larger than those which exist in corresponding co-continuous blends. These results may be caused by the encapsulated structure of those blends. Fig. 8 shows LLDPEg10/PA6 (70/30 wt/wt) where the dark PA6 phase is stained by phosphotungstic acid. The encapsulating structure (white arrows) is clearly shown. When PA6 is removed by formic acid, the encapsulated LLDPE will leave the sample and enter the acid solution. Further, there are many black droplets or small black dots dispersed in LLDPE. These droplets and micelles of PA6 may be due to interface erosion during processing [60–64]. However, the total amount of these particles is much less than the

Table 2
Weight loss of samples after extraction by selective solvent.

Sample (wt/wt)	Weight loss (wt%)	
	Extracted by formic acid	Extracted by xylene
LLDPEg10/PA6		
90/10	1.5	disintegrated
80/20	11.7	72.3 and distorted
75/25	26.1	69.8
70/30	32.7	67.9
LLDPEg5/PA6		
70/30	30.4	66.5
LLDPEg3/PA6		
70/30	16.5	disintegrated
PE-g-MAH/PA6		
70/30	8.9	disintegrated

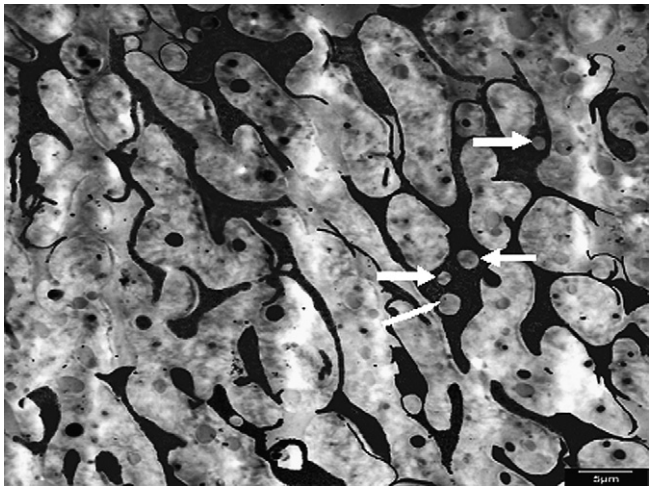

Fig. 8. TEM micrograph of LLDPEg10/PA6 (70/30 wt/wt). (PA6 was stained by phosphotungstic acid).

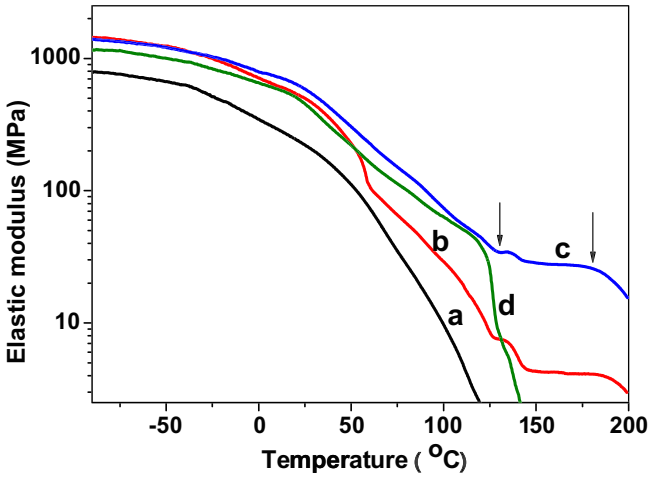

Fig. 10. Variation of elastic modulus of different LLDPEg10/PA6 and PE-g-MAH/PA6 blends obtained by DMA test: (a) 90/10, (b) 80/20, (c) 70/30, (samples a–c, PB-g-MAH content is 10 wt%); and (d) PE-g-MAH/PA6 = 70/30.

encapsulating structure in the blends. So, the extraction rate of PA6 can be higher than its real content.

Another evidence of the co-continuous morphology comes from the crystallization behavior of PA6 in different polymer blends. It is well established that semi-crystalline polymers in polymer blends with a droplet-in-matrix morphology are subjected to a fractionated crystallization process due to the lack of heterogeneous nucleating agents [36,65]. But this phenomenon will disappear when the minor phase becomes continuous [4]. Fig. 9 shows the DSC curves of different LLDPE10/PA6 blends. When the PA6 content is 10 wt% and small PA6 droplets are dispersed in LLDPE matrix (Figs. 2a and 3a), no crystallization peak of PA6 is found in the cooling curve (a). When the PA6 content is 20 wt%, a partial co-continuous morphology occurs (Figs. 2b and 3b). Referring to the cooling curve (b), part of PA6 with a larger phase size may contain normal heterogeneous nuclei and crystallizes at 185.5 °C, which is within the range of its normal crystallization temperature around 185–188 °C [36,66]. However, part of PA6 with small isolated particles containing fewer active heterogeneous nuclei may crystallize at a lower temperature (169 °C). At 30 wt%, PA6 forms a continuous phase (Figs. 2d and 3d) and the fractionated crystallization behavior vanishes. As shown in the cooling curve (c), PA crystallizes at its normal crystallization temperature.

An outstanding property induced by the co-continuous morphology is the high-temperature creep resistance. Different to the classical LLDPE/PA6 blends with a droplet-in-matrix morphology, materials with co-continuous structures suffer little creep when heated above the LLDPE melting point. For example, LLDPEg10/PA6 blends containing as much as 70 wt% LLDPE exhibit a nearly constant elastic modulus of 27 MPa between 130 and 180 °C (see the two arrows in Fig. 10c). They start to flow under stress at temperatures above which PA6 crystallites begin to melt. In contrast, for blends with a matrix-in-droplet morphology (Fig. 10a and d), the elastic modulus drops rapidly after LLDPE starts melting, even when the PA6 content is 30 wt% (Fig. 10d). But the creep resistance of LLDPEg10/PA6 (80/20) with a partial co-continuous morphology also shows a plateau modulus (2.5 MPa) after the LLDPE melting temperature (Fig. 10b). These observations are caused by the bridging effect of the PA6 domains, which has prevented flow until the melting temperature of the PA6 crystals [4].

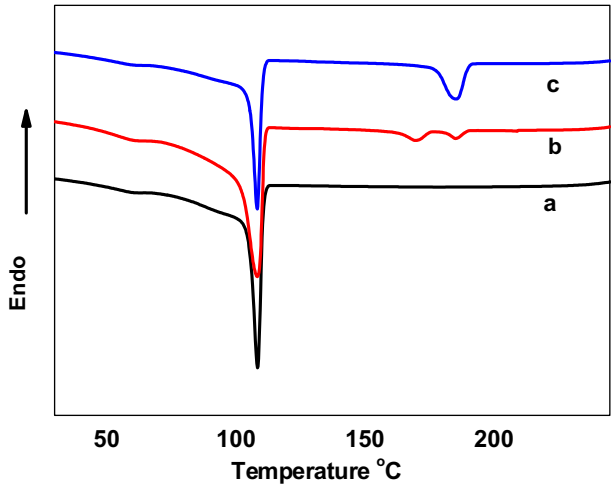

Fig. 9. DSC cooling curves of LLDPEg10/PA6 with different PA6 content: (a) 90/10; (b) 80/20; and (c) 70/30.

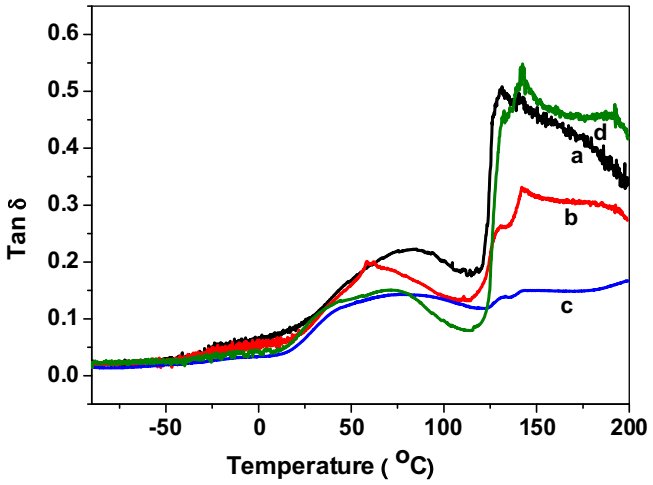

Fig. 11. . Variation of tan δ of different LLDPEg10/PA6 and PE-g-MAH/PA6 blends obtained by DMA test: (a) 90/10, (b) 80/20, (c) 70/30 (in samples a–c, PB-g-MAH content is 10 wt%); and (d) PE-g-MAH/PA6 = 70/30.

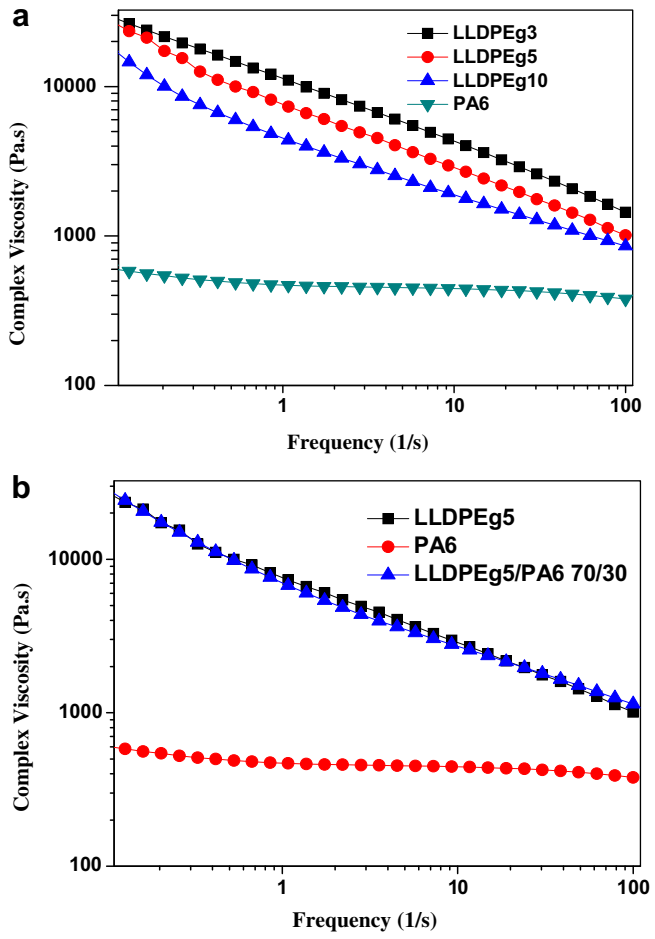

Fig. 12. (a) Shear viscosities of different components of LLDPE/PA6 blends; and (b) comparison with corresponding blends.

The tan δ *versus* temperature plots for different polymer blends also give similar results. As shown in Fig. 11, the relaxation peak at ~70 °C should be the overlap of the glass transition of PA6 and α-relaxation associated with the chain segment mobility in the LLDPE crystalline phase [67,68]. For those blends with a droplet-in-matrix morphology, there is a sharp increase in tan δ when LLDPE begins to melt (Fig. 11a and d) and the samples become viscous at this temperature. As the extent of the co-continuous structure increases, the increments of tan δ decrease sharply because the PA6 crystals can still carry the applied stress and the samples remain elastic (Fig. 11b and c).

It is generally accepted that the viscosity ratio between the dispersed phase and the matrix also has a large effect on the morphology of polymer blends [20,69]. Melt viscosity of each component in the blends studied in this work was measured by a rotation rheometer at 235 °C (which is the processing temperature of these blends). The results are shown in Fig. 12. Although the exact shear rate of the internal mixer is not known, it can be approximately estimated as the screw speed [70], which is ~50 s^{-1} for the internal mixer and 100 s^{-1} for the twin-screw extruder. It is shown in Fig. 12a that the matrix viscosities are much larger than those of the minor phase (PA6) for all the blends. The viscosity ratio, $p = \eta_d/\eta_m$, for all the blends is within 0.002–0.004. There is so little difference between p of all the blends suggesting that the viscosity ratio is not the main reason for different morphologies seen in these blends. It is well-known that when the viscosity ratio is much smaller than 1, breaking up rather than elongating and coalescing of the dispersed phase is the dominant trend and the co-continuous morphology is unfavorable to form in an uncompatibilized binary system [69]. Hence, the formation of a co-continuous morphology in these blends is due to the strong chemical reaction between the two phases and the presence of Copolymers I and II located at the interface. As shown in Fig. 12b, the viscosity of LLDPEg5/PA6 blend with 30 wt% of PA6 is similar to that of neat LLDPEg5. This phenomenon is due to the strong interface interaction between the two phases.

4. Conclusions

A facile method was used in this study to process a series of LLDPE/PA6 blends with co-continuous morphology and low PA6 contents through reactive extrusion. The co-continuous morphology was obtained by introducing simultaneously copolymers with both high and low molecular weight trunk chains to the interface. Copolymer I (LLDPE-g-PA6 or LLDPE-g-PB-g-PA6) with a high molecular weight trunk chain LLDPE strengthened the interface, favored stress transfer and induced the fine dispersion of PA6. Copolymer II (PB-g-PA6) with a low molecular weight trunk chain PB favored the formation of a flat interface between LLDPE and PA6, promoting an elongated PA6 phase. As a result, a co-continuous morphology of LLDPE/PA6 blends was successfully prepared with only 25 wt% PA6 by controlling suitable contents of Copolymers I and II in the blends. Such co-continuous morphology was maintained even after annealing at 235 °C for 0.25 h, which was stable enough for further processing. Hence, a new, facile and effective method to prepare co-continuous blends with low minor phase content via reactive extrusion has been established and proven in this work.

Acknowledgements

This study was funded by the National Science Foundation China (#50833005, #50920105302 and #50673024) and the Key project of Hubei Provincial Department of Education (D20101009). The work has also been carried out in the framework of the Research Cooperation Agreement between the Chinese Academy of Sciences (CAS) and the National Research Council (CNR) of Italy. D.S. was a Visiting Scholar to the Centre for Advanced Materials Technology (CAMT) at the University of Sydney supported by the Australian Research Council.

References

[1] Utracki LA. Commercial polymer blends. London, UK: Chapman & Hall; 1998. pp. 98.
[2] Utracki LA. Polymer alloys and blends: thermodynamics and rheology. München: Hanser Publ.; 1989. pp. 178.
[3] Paul DR, Newman S. Polymer blends, vols. 1 and 2. New York: Academic Press; 1978.
[4] Pernot H, Baumert M, Court F, Leibler L. Nat Mater 2002;1(1):54–8.
[5] Mamat A, Vu Khanh T, Cigana P, Favis BD. J Polym Sci Part B Polym Phys 1997;35(16):2583–92.
[6] Niebergall U, Bohse J, Schürmann BL, Seidler S, Grellmann W. Polym Eng Sci 1999;39(6):1109–18.
[7] Flexman EA, Huang DD, Snyder HL. Polymer Preprints. American Chemical Society. Division of polymer chemistry, Papers presented at the Los Angeles, CA Meeting; September, 1988, vol. 29(2):189–190.
[8] Sarazin P, Favis BD. Biomacromolecules 2003;4(6):1669–79.
[9] Li J, Favis BD. Polymer 2001;42(11):5047–53.
[10] Yang SY, Yu IR, Kim HY, Kim JK, Jang SK, Russell TP. Adv Mater 2006;18(6):709–12.
[11] Salehi P, Sarazin P, Favis BD. Biomacromolecules 2008;9(4):1131–8.
[12] Sperling LH. Interpenetrating polymer networks: an overview. In: Klempner D, Sperling LH, Utracki LA, editors. Interpenetrating polymer networks. Adv Chem Ser, vol. 239; 1994. p. 5. Washington.
[13] Sperling LH. An introduction to polymer networks and IPNs. In: Interpenetrating polymer networks and related materials. New York and London: Plenum Press; 1981. p. 1–30.
[14] Kim JK, Taki K, Nagamine S, Ohshima M. Langmuir 2008;24(16):8898–903.

[15] Higgins AM, Jones RA. Nature 2000;404:476–8.
[16] Riscanu D, Favis BD, Feng CY, Matsuura T. Polymer 2004;45(16):5597–609.
[17] Rovere AD, Grady BP, Shambaugh RL. J Appl Polym Sci 2002;83(8):1759–72.
[18] Béquet S, Remigy JC, Rouch JC, Espenan JM, Clifton M, Aptel P. Desalination 2002;144(1–3):9–14.
[19] Avgeropoulos GN, Weissert FC, Biddison PH, Böhm GGA. Rubber Chem Technol 1976;49(1):93–104.
[20] Paul DR, Barlow JW. J Macromol Sci Rev Macromol Chem Phys 1980;C18 (1):109–68.
[21] Jordhamo GM, Manson JA, Sperling LH. Polym Eng Sci 1986;26(8):517–24.
[22] Veenstra H, van Lent BJJ, van Dam J, Posthuma de Boer A. Polymer 1999;40 (24):6661–72.
[23] Veenstra H, van Dam J, Posthuma de Boer A. Polymer 1999;40(5):1119–30.
[24] Veenstra H, van Dam J, Posthuma de Boer A. Polymer 2000;41(8):3037–45.
[25] Scott CE, Macosko CW. Polymer 1995;36(3):461–70.
[26] Sundararaj U, Dori Y, Macosko CW. Polymer 1995;36(10):1957–68.
[27] Willemse RC, Posthuma de Boer A, van Dam J, Gotsis AD. Polymer 1998;39 (24):5879–87.
[28] Willemse RC, Posthuma de Boer A, van Dam J, Gotsis AD. Polymer 1999;40 (4):827–34.
[29] Zhang CL, Feng LF, Zhao J, Huang H, Hoppe S, Hu GH. Polymer 2008;49 (16):3462–9.
[30] Utracki LA. PE/PP blends. In: Commercial polymer blends. London: Chapman & Hall; 1998. p. 255–8.
[31] Yuan ZH, Favis BD. AIChE J 2005;51(1):271–80.
[32] Marin N, Favis BD. Polymer 2002;43(17):4723–31.
[33] Bhadane PA, Champagne MF, Huneault MA, Tofan F, Favis BD. Polymer 2006;47(8):2760–71.
[34] Hellmann GP, Dietz M, Fischer M. J Macromol Sci Phys 1996;35(3):477–88.
[35] Jiang M, Cao X, Yu T. Polymer 1986;27(12):1923–7.
[36] Shi D, Yin J, Ke Z, Gao Y, Li RK. J Appl Polym Sci 2004;91(6):3742–55.
[37] Yang J, Shi D, Gao Y, Song Y, Yin J. J Appl Polym Sci 2003;88(1):206–13.
[38] Macosko CW, Jeon HK, Hoye TR. Prog Polym Sci 2005;30(8–9):939–47.
[39] Jeon HK, Zhang J, Macosko CW. Polymer 2005;46(26):12422–9.
[40] Cigana P, Favis BD, Jerome R. J Polym Sci Part B Polym Phys 1996;34 (9):1691–700.
[41] Lyu S, Jones TD, Bates FS, Macosko CW. Macromolecules 2002;35(20):7845–55.
[42] Bates FS, Maurer WW, Lipic PM, Hillmyer MA, Almdal K, Mortensen K, et al. Phys Rev Lett 1997;79(5):849–52.
[43] Hillmyer MA, Maurer WW, Lodge TP, Bates FS, Almdal K. J Phys Chem B 1999;103(23):4814–24.
[44] Ruzette AV, Leibler L. Nat Mater 2005;4(1):19–31.
[45] Hamley IW, Koppi KA, Rosedale JH, Bates FS, Almdal K, Mortensen K. Macromolecules 1993;26(22):5959–70.
[46] Foerster S, Khandpur AK, Zhao J, Bates FS, Hamley IW, Ryan AJ, et al. Macromolecules 1994;27(23):6922–35.
[47] Pu G, Luo Y, Lou Q, Li B. Macromol Rapid Commun 2009;30(2):133–7.
[48] Brown HR, Char K, Deline VR, Green PF. Macromolecules 1993;26 (16):4155–63.
[49] Milner ST. Macromolecules 1994;27(8):2333–5.
[50] Pochan DJ, Gido SP, Pispas S, Mays JW, Ryan AJ, Fairclough JPA, et al. Macromolecules 1996;29(15):5091–8.
[51] Meng T, Gao X, Zhang J, Yuan J, Zhang Y, He J. Polymer 2009;50(2):447–54.
[52] Liu W, Liu R, Li Y, Kang H, Shen D, Wu M, et al. Polymer 2009;50(1):211–7.
[53] Shi D, Ke Z, Yang J, Gao Y, Wu J, Yin J. Macromolecules 2002;35(21):8005–12.
[54] Leibler L. Macromolecules 1982;15(5):1283–90.
[55] Noolandi J, Hong KM. Macromolecules 1982;15(2):482–92.
[56] Fayt R, Teyssie P. Macromolecules 1986;19(7):2077–80.
[57] Hobbs SY, Dekkers MEJ, Watkins VH. J Mater Sci 1989;24(6):2025–30.
[58] Zhang CL, Feng LF, Gu XP, Hoppe S, Hu GH. Polymer 2007;48(20):5940–9.
[59] Shi D, Yang J, Yao Z, Wang Y, Huang H, Wu J, et al. Polymer 2001;42 (13):5549–57.
[60] Bhadane PA, Tsou AH, Cheng J, Favis BD. Macromolecules 2008;41(20):7549–59.
[61] Jabbarzadeh A, Atkinson JD, Tanner RI. Macromolecules 2003;36 (13):5020–31.
[62] Charoensirisomboon P, Inoue T, Weber M. Polymer 2000;41(18):6907–12.
[63] Pan L, Chiba T, Inoue T. Polymer 2001;42(21):8825–31.
[64] Pan L, Inoue T, Hayami H, Nishikawa S. Polymer 2002;43(2):337–43.
[65] Arnal ML, Matos ME, Morales RA, Santana OO, Müller AJ. Macromol Chem Phys 1998;199(10):2275–88.
[66] Tol RT, Mathot VBF, Reynaers H, Goderis B, Groeninckx G. Polymer 2005;46 (9):2966–77.
[67] John B, Varughese KT, Oommen Z, Pötschke P, Thomas S. J Appl Polym Sci 2003;87(13):2083–99.
[68] Ward IM, Sweeney J. An introduction to the mechanical properties of solid polymers. 2nd ed. New York: Wiley-Interscience; 2004.
[69] Everaert V, Aerts L, Groeninckx G. Polymer 1999;40(24):6627–44.
[70] Wu S. Polym Eng Sci 1987;27(5):335–43.